


ORIGINAL RESEARCH

Metabolomics analysis reveals distinct profiles of nonmuscle-invasive and muscle-invasive bladder cancer

Divya Sahu¹, Yair Lotan², Bryan Wittmann³, Bruce Neri³ & Donna E. Hansel¹ ¹Department of Pathology, University of California at San Diego, La Jolla, California²Department of Urology, University of Texas Southwestern Medical Center, Dallas, Texas³Metabolon Inc., Durham, North Carolina**Keywords**

Gas chromatography, liquid chromatography, mass spectrometry, metabolic networks and pathways, metabolomics, urinary bladder neoplasms, urothelium

Correspondence

Donna E. Hansel, Department of Pathology, University of California at San Diego, 9500 Gilman Drive, MC 0612, La Jolla, CA 92093. Tel: 858-534-1716; Fax: 858-534-8852; E-mail: dhansel@ucsd.edu

Funding Information

This work was supported by the Case Western Reserve University/Cleveland Clinic CTSA Grant Number UL1 RR024989 from the National Center for Research Resources (NCRR) and a KL2 career development award (RR024990) to D.E.H., as well as a Prevent Cancer Foundation Fellowship Award to D.S.

Received: 5 February 2017; Revised: 21 April 2017; Accepted: 1 May 2017

Cancer Medicine 2017; **6**(9):2106–2120

doi: 10.1002/cam4.1109

Introduction

Bladder cancer affects more than 400,000 patients worldwide annually [1, 2]. The majority of cases consist of noninvasive low-grade and high-grade urothelial carcinoma (Ta, Tis) and early invasive urothelial carcinoma (T1), collectively termed nonmuscle-invasive bladder cancer (NMIBC). Whereas low-grade papillary urothelial carcinoma progresses only in a minority of patients, those with high-grade Ta, Tis, or T1 disease have a markedly increased risk of progression. Patients with NMIBC are treated with transurethral resection (TURBT) and, for high-grade disease, with intravesical therapy that includes Bacillus Calmette-Guérin (BCG, modified mycobacterium

Abstract

Urothelial carcinoma is the most common form of bladder cancer, but pathway changes that occur with stage-wise progression have not been well defined. We used a metabolomics approach to identify potential metabolic pathways uniquely altered in normal urothelium, nonmuscle-invasive bladder cancer (NMIBC), and muscle-invasive bladder cancer (MIBC). We performed global metabolomic profiling using GC-mass spectrometry (MS) and LC-MS platforms to identify metabolite signatures between normal urothelium and high-grade urothelial carcinoma of different stages. Pathways globally dysregulated in cancer relative to normal urothelium included glucose, tricarboxylic acid (TCA) cycle, lipid, amino acid, and nucleotide pathways. Urothelial carcinoma showed elevated glucose utilization for glycolysis and increased sorbitol pathway intermediates, consistent with Warburg effect. Anaplerosis to sustain energy production suggested by increased late TCA cycle intermediates, amino acids, and dipeptides occurs in bladder cancer. Urothelial carcinoma also shows altered membrane lipid membrane metabolism and differential derivation of nucleic acid components pyrimidine and purine. In stage comparison, MIBC appears to preferentially enhance cyclooxygenase (COX) and lipoxygenase (LOX) signaling, increase heme catabolism, and alter nicotinamide adenine dinucleotide (NAD⁺) synthesis with a possible influence from associated inflammatory cells. We identify numerous metabolomic alterations in NMIBC and MIBC that likely reflect underlying pathway changes. Differential pathway activity may have value in designing stage-specific novel therapeutics in urothelial carcinoma.

[3]. Although BCG can be effective to delay or prevent disease progression in a subset of patients, a significant proportion of patients ultimately develop invasive disease. Moreover, given the recent global shortage of BCG, there is a need for alternative, rational therapies in this population. In contrast, the primary treatment for patients with muscle-invasive bladder cancer (MIBC) includes radical cystectomy and bilateral regional lymph node dissection with or without neoadjuvant chemotherapy or chemoradiation.

One approach to identify differentially activated and potentially actionable pathways in these different patient populations is metabolomic profiling. Metabolomic signatures, which reflect the overall biological activity inherent

in each cancer, may be used to detect unique pathways activated in cancer subtypes and has been applied to breast, ovarian, head and neck, colorectal, and hepatocellular carcinomas [4]. Prior studies using metabolomic analysis of bladder cancer have focused primarily on screening and detection applications using urine [5], serum [6], and cell culture [7]. Several additional studies have identified differences between normal urothelium and neoplastic bladder tissue and have identified a subset of metabolites that appear to be unique in these populations [4, 8, 9].

In our study, we have used a unique and highly sensitive approach to expand the identification of altered metabolites in bladder cancer. We have also included high-grade urothelial carcinomas of different stages to identify unique signatures that distinguish NMIBC from MIBC, given that these two populations undergo markedly different treatment paradigms and may require distinct pathway-based approaches when designing new therapies. The results from our analysis show numerous pathways uniquely altered between high-grade NMIBC and MIBC that may serve as the basis for development of alternative therapies.

Materials and Methods

Patient specimens

Patient tissue samples were obtained with approval by participating institution institutional review boards. High-grade urothelial carcinoma without variant morphology was obtained from 72 patients, with matched histologically normal urothelium also obtained from 24 patients. Seven additional benign samples from patients without urothelial neoplasia history were collected. Samples were snap-frozen, de-identified, and stored at -80°C , and a frozen section was obtained to verify diagnosis and presence of $>80\%$ tumor nuclei. Demographic and prior treatment history was collected from patient record review. Detailed patient characteristics are described in Table 1. Samples were shipped via cryovial to Metabolon Inc (Durham, NC) for analysis. The analytical group was blinded to sample subgroup, and samples were, therefore, randomized on the platform for analysis.

Cell culture

T24, J82 and UM-UC-3 cell lines were purchased from the American Type Culture Collection (ATCC, Manassas, VA). UROtsa cells were obtained from Deutsche Sammlung für Mikroorganismen und Zellkultur (Braunschweig, Germany). Cells were grown in RPMI-1640 (GIBCO, Life Technologies, Grand Island, NY) supplemented with 10% fetal bovine serum (GIBCO).

Metabolomic profiling

The mass spectrometer platforms, sample extraction and preparation, instrument settings and conditions, and data handling have been described in detail [5]. In brief, weight-normalized tissue extract containing a cocktail of recovery standards was divided into three fractions for untargeted metabolic profiling and randomized for analysis that included the following: ultrahigh-performance liquid chromatography/tandem mass spectrometry (UHPLC-MS/MS) in the negative ion mode, UHPLC-MS/MS in the positive ion mode, and gas chromatography-mass spectrometry (GC-MS) after silylation. Reproducibility was assessed by the recovery of the xenobiotic compounds spiked in every sample prior to extraction. The samples were analyzed using a platform consisting of a Waters ACQUITY UHPLC (Waters Corporation, Milford, MA, USA) and a Thermo-Finnigan LTQ mass spectrometer (Thermo Fisher Scientific Inc., Waltham, MA, USA). The data extraction of the raw mass spec data files yielded information that could be loaded into a relational database and manipulated without resorting to BLOB manipulation. Once in the database, the information was examined and appropriate quality control limits were imposed. Peaks were identified using Metabolon's proprietary peak integration software, and component parts were stored in a separate and specifically designed complex data structure. Compounds were identified by comparison to library entries of purified standards or recurrent unknown entities. Identification of known chemical entities was based on comparison to metabolomic library entries of purified standards. As of this writing, more than 2000 commercially available purified standard compounds had been acquired and registered into the LIMS for distribution to both the LC and GC platforms for determination of their analytical characteristics. The combination of chromatographic properties and mass spectra gave an indication of a match to the specific compound or an isobaric entity. Additional entities (unnamed compounds) were identified by their recurrent chromatographic and mass spectral signature and have the potential to be identified by future acquisition of a matching purified standard or by classical structural analysis. A variety of curation procedures were carried out to ensure that a high-quality data set was made available for statistical analysis and data interpretation. The quality control and curation processes were designed to ensure accurate and consistent identification of true chemical entities and to remove those representing system artifacts, misassignments, and background noise. Proprietary visualization and interpretation software were used by Metabolon to confirm the consistency of peak identification among the various samples. Library matches for each compound were checked for each sample and corrected if necessary. For studies spanning multiple days, a data normalization step was performed to

Table 1. Patient demographics and precedent therapy.

Cohort 1: Benign versus neoplastic comparison						
Metabolic Pathway	Normal	Nonmuscle invasive		Muscle invasive		
		Ta	T1	T2	T3	T4
Number of patients	7	5	3	2	10	4
Mean age	69.7	69.7	67.2	59.3	66.2	66.7
Gender ¹						
Male	5	5	3	2	8	4
Female	2	0	0	0	2	0
Race						
Caucasian	5	3	2	2	10	4
African-American	2	0	0	0	0	0
Other	0	2	1	0	0	0
Prior BCG treatment		1	0	0	2	0
Prior neoadjuvant chemo ²		0	1	0	2	2

Cohort 2: High-grade NMIBC versus MIBC comparison					
Metabolic pathway	Nonmuscle invasive		Muscle invasive		
	High grade Ta	T1	T2	T3	T4
Number of patients	7	10	7	19	5
Mean age	67.6	69.7	74.3	64.3	68.4
Gender ¹					
Male	6	8	7	15	2
Female	1	2	0	4	3
Race					
Caucasian	7	8	5	18	5
African-American	0	2	1	1	0
Other	0	0	1	0	0
Prior BCG treatment	1	3	0	4	0
Prior neoadjuvant chemo ²	0	0	0	0	0

¹Fishers exact test $P = 0.3143$.

²Fishers exact test $P = 0.0030$.

correct variation resulting from instrument inter-day tuning differences. Essentially, each compound was corrected in run-day blocks by registering the medians to equal one (1.00) and normalizing each data point proportionately (termed the “block correction”). For studies that did not require more than 1 day of analysis, no normalization is necessary, other than for purposes of data visualization.

Statistical analysis

All statistical analyses were performed in R version 2.14.2 (<http://cran.r-project.org/>). Wilcoxon test and matched-pair t-tests were used to determine statistical significance of metabolite mean differences between comparator groups (see Fig. 1 for statistical comparisons). For all analyses, missing values (if any) were imputed with the observed minimum for that particular compound (imputed values were added after block normalization).

The statistical analyses were performed on natural log-transformed data to reduce the effect of any potential outliers in the data. To account for false positives in multiple comparison testing, q-values were utilized to estimate the false discovery rate (FDR) for a specific comparator group.

Immunoblot analysis

Whole cell lysates were extracted with RIPA buffer containing protease and phosphatase inhibitor cocktails (Roche, Basel, Switzerland) and subjected to Western blot analysis as previously described [10]. Proteins were separated on 4–15% gradient polyacrylamide–sodium dodecyl sulfate gels (Bio-rad Laboratories, Inc., Hercules, CA), transferred to Supported Nitrocellulose membranes (Bio-rad) using a Bio-Rad Mini-PROTEAN Tetracell system, followed by incubation for 1 h in a bovine serum

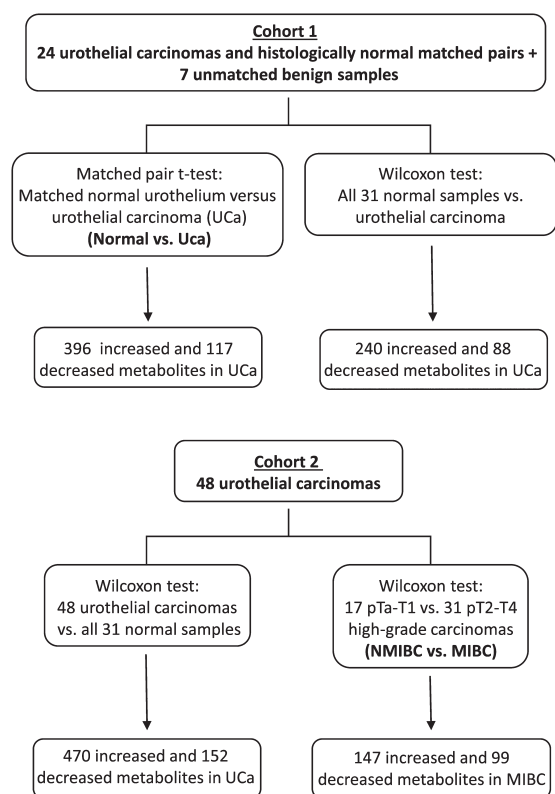


Figure 1. Schematic of statistical analysis using two patient cohorts of urothelial carcinoma.

albumin-Tween-20-based blocking solution. Primary antibodies were Hexokinase I (1:1000), Hexokinase II (1:1000), phosphofruktokinase (PFK) (1:1000), pyruvate kinase M1/2 isoform (PKM1/2) (1:1000), pyruvate kinase M2 isoform (PKM2) (1:1000), pyruvate dehydrogenase (PDH) (1:1000), lactate dehydrogenase A (LDHA) (1:1000), GAPDH (1:1000), and actin (1:1000), all from Cell Signaling Technology, Inc. (Danvers, MA). Blots were incubated with primary antibody overnight and then incubated for 1 h with horseradish phosphatase-conjugated anti-rabbit or anti-mouse secondary antibodies (1:10,000; Jackson ImmunoResearch Laboratories, Inc., West Grove, PA). Blots were developed using the Enhanced Chemiluminescence Kit (Pierce, Thermo Fisher Scientific, Waltham, MA) followed by autoradiography.

Results

Uniquely altered metabolites between histologically normal urothelium and high-grade bladder cancer

To identify differences between normal-appearing urothelium and high-grade urothelial cancer, we used 24 matched

specimens and an additional seven cases of true benign urothelium. In total, 513 metabolites were altered between normal and neoplastic tissue (matched pair t-test, $P \leq 0.05$, FDR 3.3%), and these results held true in larger cohort of 48 urothelial carcinoma specimens, with the exception of 5 dipeptides. A detailed summary of cohort comparisons is shown in Figure 1.

Glucose metabolism shows a shift to glycolysis and increased shunting toward sorbitol pathway in urothelial carcinoma

A preferential shift to aerobic glycolysis (Warburg effect) occurs in many cancers, resulting in reduced glucose levels and increased pyruvate and lactate levels, among other changes [11]. In contrast with normal urothelium, urothelial carcinoma showed a Warburg effect with significantly low glucose ($P = 0.0004$) and nonsignificant increased glucose-6-phosphate (G6P), fructose-6-phosphate (F6P), fructose-1,6-bisphosphate (F1,6bisP), pyruvate, and lactate levels (Fig. 2). We validated a subset of the enzymes involved in this pathway by immunoblot analysis using a panel of bladder cells including the normal immortalized UROtsa cell line and the invasive T24, J82, and UM-UC-3 lines. Hexokinase II, PFK, PDH, and LDHA protein expression are increased in invasive bladder cancer cells compared with UROtsa cells (Fig. S1).

Rather than continuing on the glycolytic pathway, the G6P metabolite can instead be routed to the pentose phosphate pathway (PPP) for regeneration of reduced nicotinamide adenine dinucleotide phosphate (NADPH) to maintain redox status. Although slight increases in late PPP intermediates such as ribulose-5-phosphate (Ru5P), sedoheptulose-7-phosphate (S7P), and fructose-6-phosphate (F6P) were observed, only the end-product ribose was significantly increased in neoplastic urothelium ($P = 0.0008$), suggesting activation of the PPP pathway. Glucose may also be shunted into the sorbitol pathway, which appears to be enhanced in urothelial neoplasia as well, with nonsignificant elevation of sorbitol and significantly increased downstream derivatives fructose ($P = 0.0001$) and fructose-1-phosphate ($P = 0.0028$).

Increased late-stage TCA cycle intermediates indicate anaerobic activity in urothelial carcinoma

Pyruvate generated by glycolysis enters mitochondria for conversion to acetyl-CoA, which then reacts with oxaloacetate to form citrate. Citrate can proceed through the TCA cycle or alternatively be transported to the cytoplasm

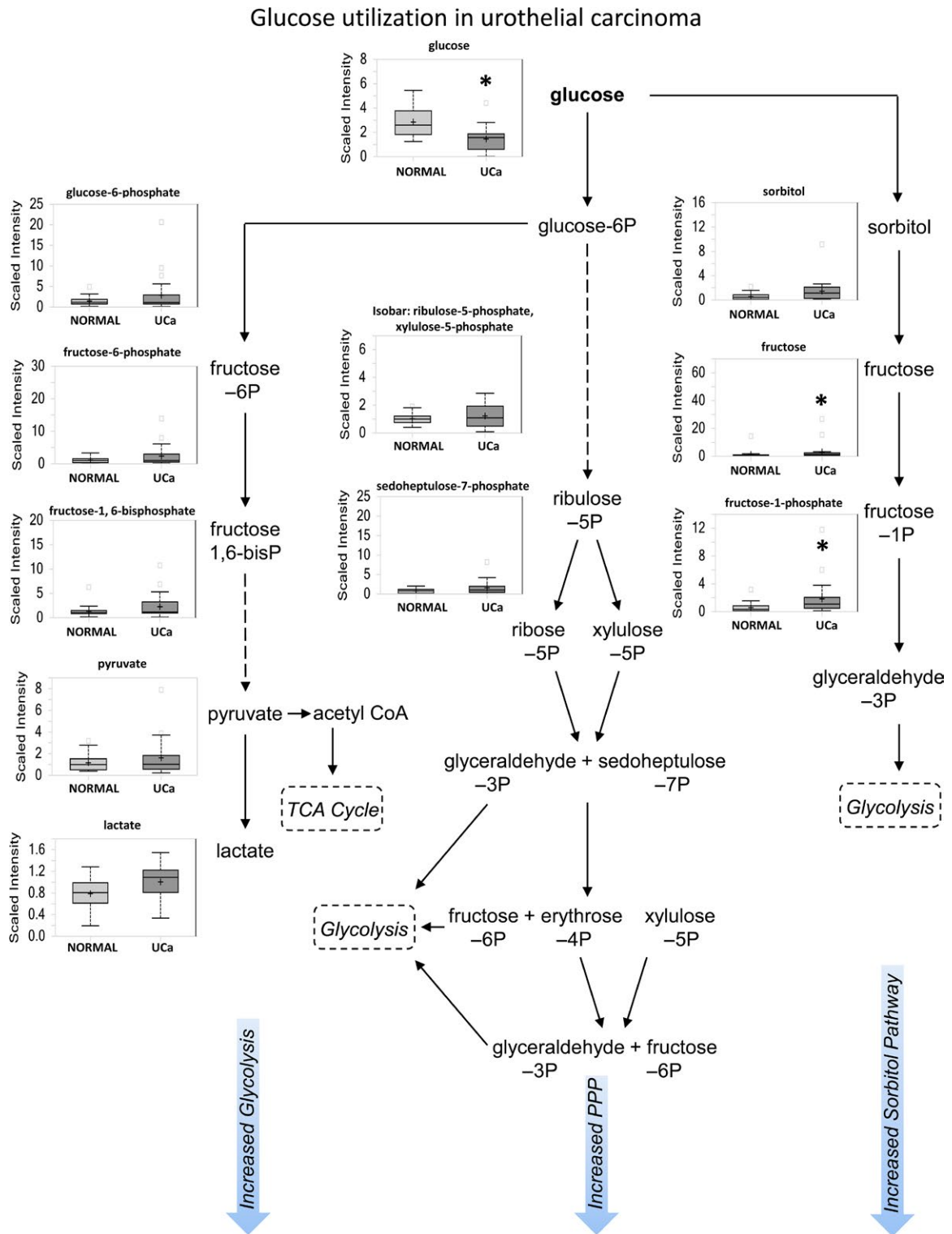


Figure 2. Glucose metabolism shows an increase in glycolysis, sorbitol, and PPP pathway activity in urothelial carcinoma. Box plots show a comparison between histologically normal urothelium (NORMAL) and urothelial carcinoma (UCa) matched pairs. This schematic shows glucose utilization pathways that include glycolysis, PPP, and sorbitol pathways.

Increased late stage TCA cycle intermediates in urothelial carcinoma suggest anaplerosis

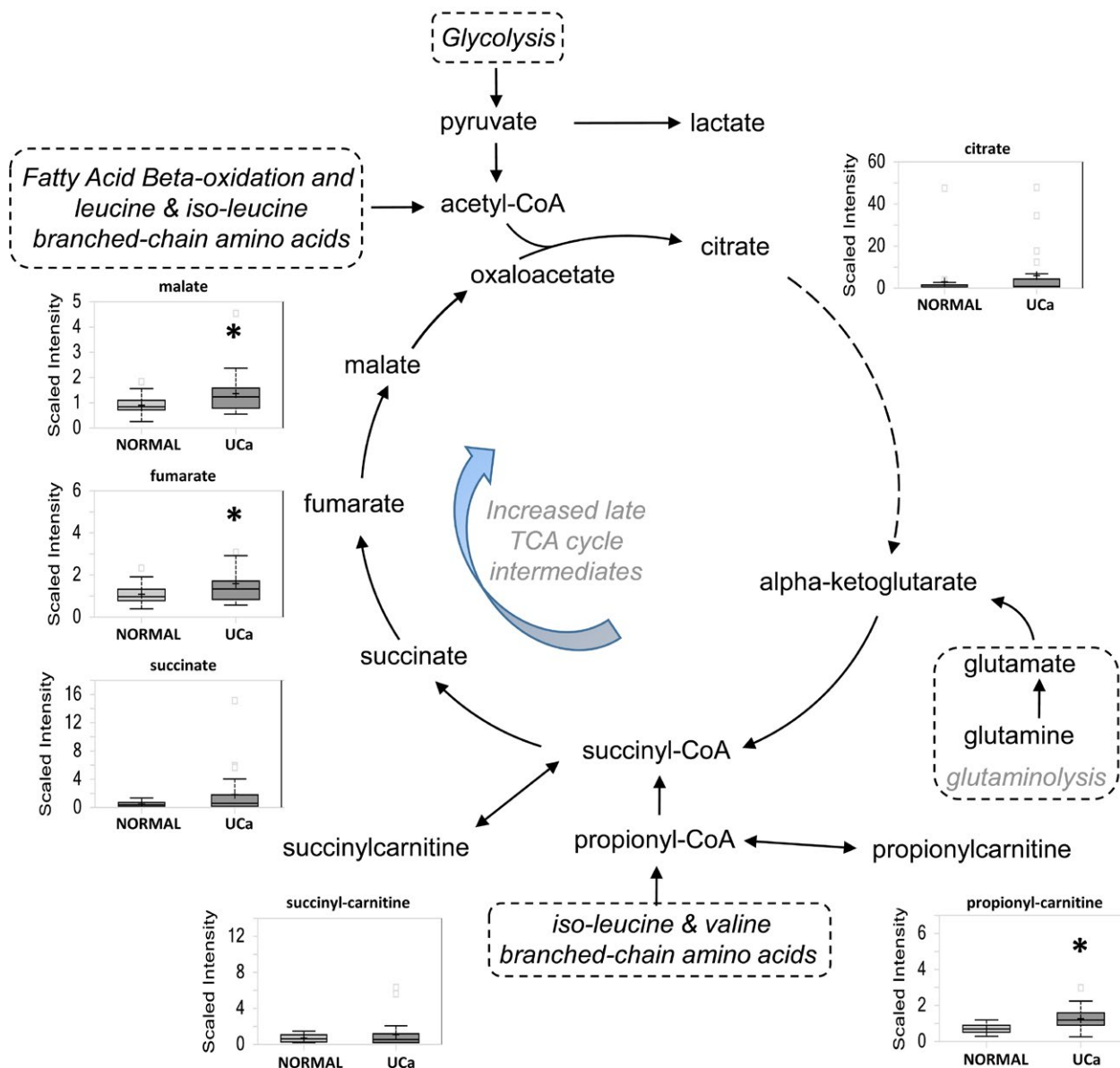
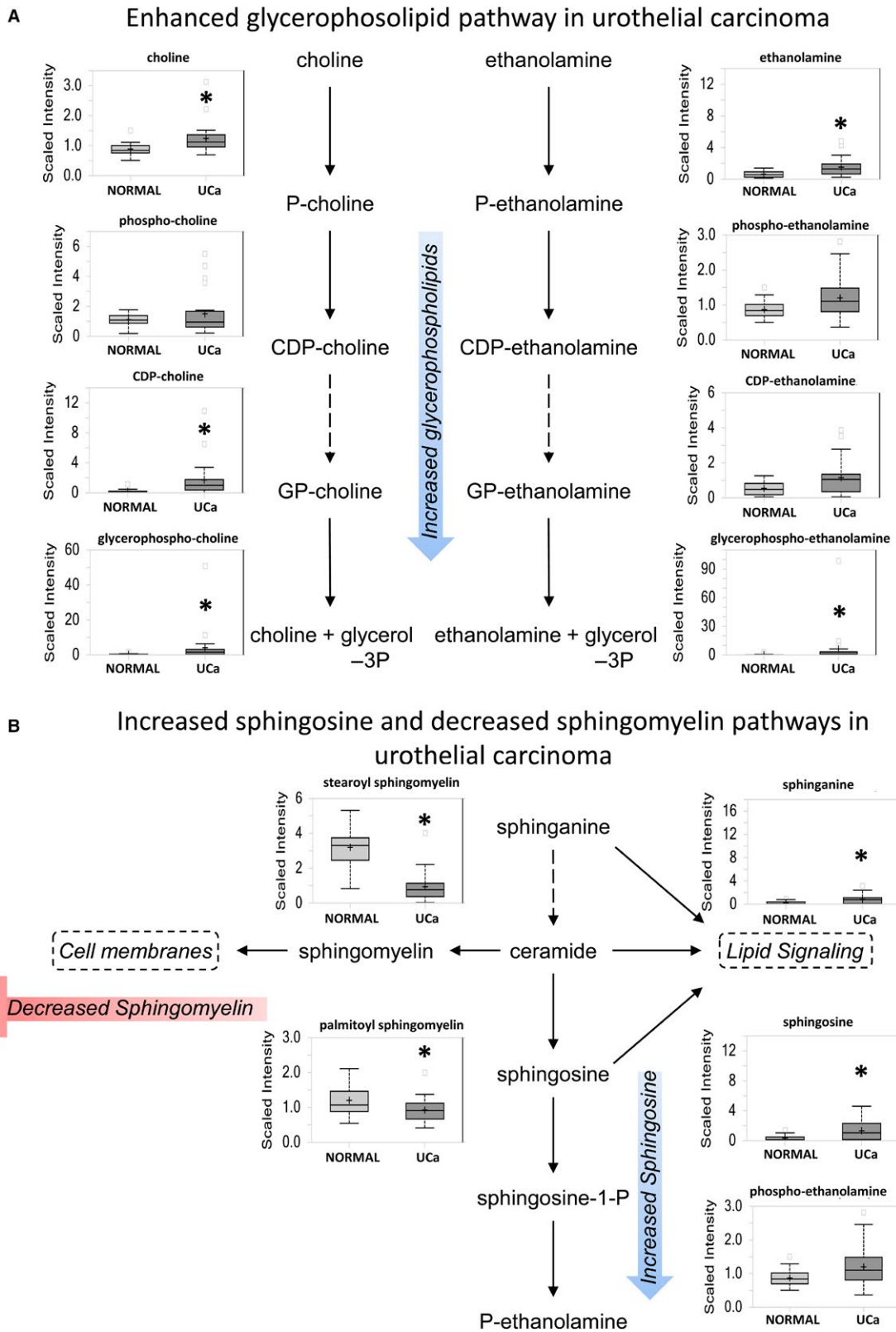


Figure 3. Increased late-stage TCA cycle intermediates suggest the potential for increased anaplerotic activity to sustain energy production in urothelial carcinoma. Elevations in metabolites are seen in carcinoma specimens suggest a potential role for anaplerosis in UCa.

for fatty acid synthesis. We identify significant increases in late TCA cycle intermediates fumarate ($P = 0.0269$) and malate ($P = 0.0249$) and nonsignificant increase in citrate and succinate in urothelial carcinoma (Fig. 3). This increase, when coupled with higher levels of amino acids described later in this study, suggests anaplerotic activity may occur in urothelial carcinoma as a mechanism to sustain energy production.

Lipid metabolism shows formation of fatty acids, glycerophospholipids, and sphingolipids in urothelial carcinoma

Urothelial carcinoma shows significant upregulation of multiple lipid classes in contrast with normal urothelium that include medium chain, long chain, polyunsaturated and branched fatty acids, monoacylglycerols, lysolipids, and



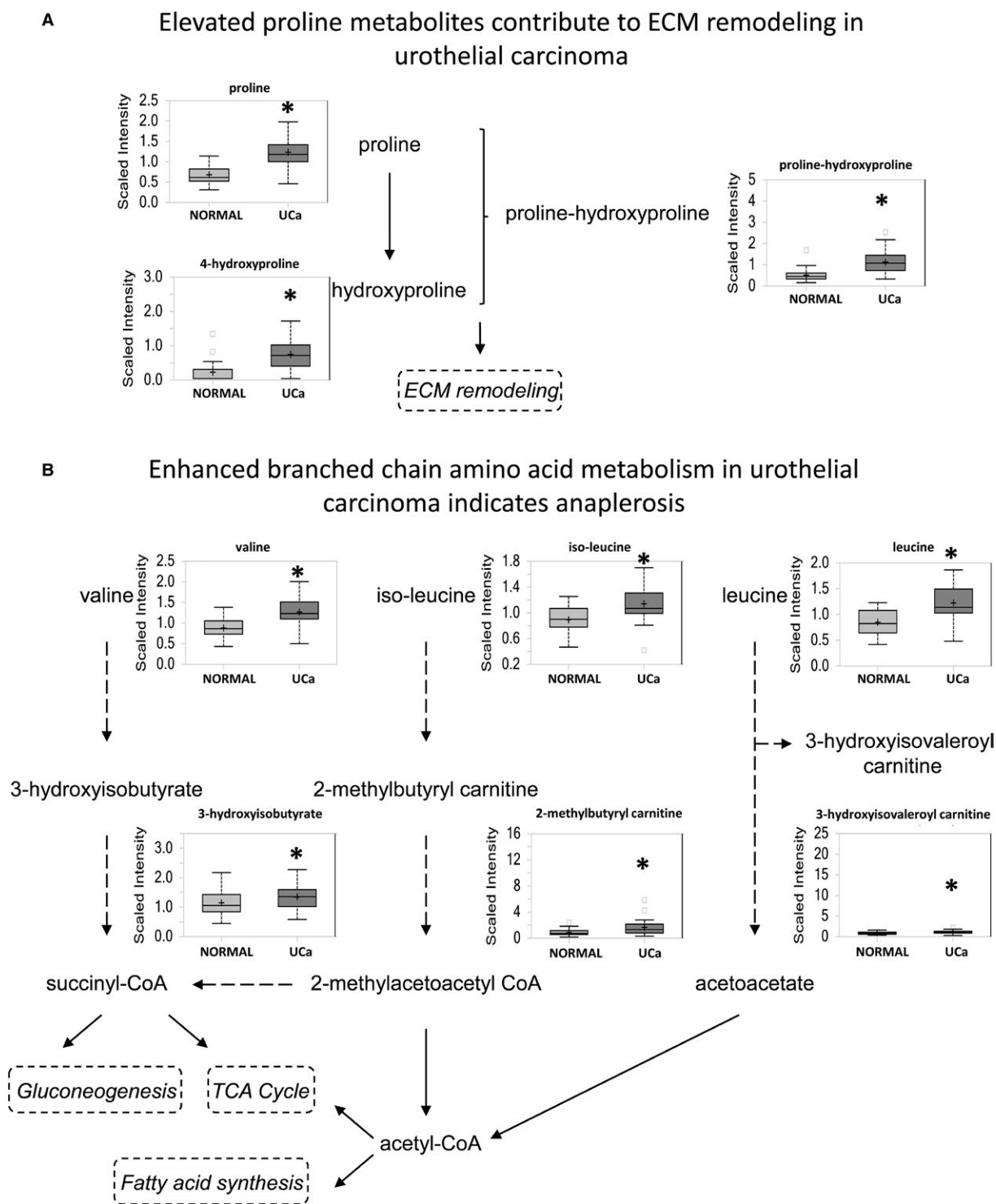


Figure 5. Elevated amino acid metabolism supports the potential role of anaplerosis in urothelial carcinoma energy production. (A) One of the highest increases were seen with proline which is a component of the ECM. (B) Increased production of branched chain amino acids valine, iso-leucine, and leucine was seen.

endocannabinoids ($P < 0.05$ for all classes). Significant elevations of glycerophospholipids (Fig. 4A) and sphingolipids (Fig. 4B), which are critical components of cell membrane

biosynthesis and turnover during cell proliferation, were present in urothelial carcinoma. The significant increase in sphinganine ($P = 0.0149$) and sphingosine ($P = 0.0364$),

Table 2. Alterations in purine metabolites.

Class	Metabolite	Carcinoma:normal ratio	P-value
Bases	Xanthine	2.01	0.0003
	Hypoxanthine	1.42	0.0008
	Adenine	1.04	0.1697
	Guanine	1.76	0.8688
Nucleosides	Xanthosine	1.09	0.3383
	Inosine	0.7	0.0018
	2'-deoxyinosine	3.42	7.72E-05
	Adenosine	0.6	0.0434
	Guanosine	0.77	0.0122
	2'-deoxyguanosine	1.9	0.0007
Nucleotides	Inosine 5'-monophosphate	0.84	0.3246
	Adenosine 2'-monophosphate	2.72	0.0008
	Adenosine 3'-monophosphate	4.64	6.50E-06
	Adenosine 5'-monophosphate	1.3	0.7892
	Adenosine 5'-diphosphate	0.65	0.07
	Guanosine 5'-monophosphate	2.42	0.4561
Methylated	Guanosine 3'-monophosphate	5.8	4.05E-05
	N1-methyladenosine	1.68	0.0005
	7-methylguanine	1.88	7.51E-05
	N1-methylguanosine	3.7	2.28E-07
	N2-methyladenosine	2.03	4.72E-05
Biosynthesis	N2, N2-dimethylguanosine	2.67	1.04E-06
	AICA ribonucleotide	2	0.0078
Catabolism	Adenylosuccinate	6.22	0.0044
	Urate	1.59	0.7592
	Allantoin	3.32	0.9491

with concurrent significant decrease in sphingomyelin derivatives stearoyl sphingomyelin ($P = 8.52E-07$) and palmitoyl sphingomyelin ($P = 0.0069$) suggests preferential conversion of ceramide to sphingosine in cancer cells (Fig. 4B).

Additional upregulated long-chain acyl-carnitines include propionylcarnitine, valerylcarnitine, and deoxycarnitine, which, when combined with a slight increase of ketone body beta-hydroxybutyrate (BHBA) and decreased dicarboxylic fatty acids, suggest efficient beta-oxidation of fatty acids in urothelial carcinoma.

Elevated amino acid metabolism also supports a potential anaplerotic mechanism in urothelial carcinoma

Most amino acids were significantly elevated in urothelial carcinoma, with highest increases in proline ($P = 5.92E-09$), alanine ($P = 1.09E-05$), and asparagine ($P = 2.60E-06$). Increased amino acid levels reflect either increased protein breakdown within cancer cells or increased uptake of amino acids into cancer cells from the microenvironment. Proline and its derivatives are important constituents of collagen, which makes up the extracellular matrix, and were significantly upregulated in urothelial carcinoma (Fig. 5A). Other extracellular matrix-related metabolites were also increased,

including glucosamine ($P = 0.0118$), N-acetylglucosamine ($P = 0.0003$), N-acetylglucosamine 6-phosphate ($P = 0.0007$), N-acetylgalactosamine ($P = 6.95E-06$), N-acetylneuraminic acid ($P = 2.25E-05$), fucose ($P = 0.0075$), erythronate ($P = 5.84E-05$), glucuronate ($P = 0.0142$), and UDP-glucuronate ($P = 0.0157$), which may indicate active extracellular matrix remodeling in the context of carcinoma development and/or progression. Furthermore, nutrient stress can promote alpha-ketoglutarate and glutamate formation by proline shunting to proline oxidase, which contributes to anaplerosis [12, 13].

Branched-chain amino acid metabolism was also increased in urothelial carcinoma, including increased leucine ($P = 3.80E-06$), isoleucine ($P = 0.0002$), valine ($P = 2.07E-07$), and their degradation products (Fig. 5B). Enhanced catabolism and anaplerosis may contribute to the observed changes in the late TCA intermediates, supported by higher levels of propionylcarnitine.

Purine/pyrimidine metabolism shows enhanced production of deoxy-nucleotides and derivation of purine from de novo synthesis and catabolism in cancer

Both purine and pyrimidine metabolites were increased in urothelial carcinoma, which, when combined with

increased catabolic products, suggests increased degradation of nucleic acids (Table 2). Methylated nucleobases were also globally increased and may be caused by either enhanced nucleic acid turnover or increased methylation [14]. Purine levels are increased due to both, de novo synthesis and catabolism of nucleotides. The decreased levels of adenosine, inosine, and guanosine, coupled with elevated levels of guanine, hypoxanthine, and xanthine, could be the result of potentially elevated xanthine oxidase levels leading to increased oxidative stress [15]. Most bases, nucleosides, and nucleotides of the pyrimidine metabolic pathway were also increased in urothelial carcinoma.

Differential metabolites between nonmuscle-invasive and muscle-invasive urothelial carcinoma suggest possible uniquely actionable pathways

We compared data between NMIBC and MIBC using 48 pathologically staged samples (Fig. 1). Overall 246 metabolites were distinctly present between NMIBC and MIBC samples (Wilcoxon test, $P \leq 0.05$, FDR 11.3%).

Elevated prostaglandin and thromboxane levels occur in pathologically advanced disease

Eicosanoids such as prostaglandins, thromboxanes, and leukotrienes are biologically active signaling components of the COX and LOX pathways. Elevated prostaglandin A2 ($P = 0.002$), B2 ($P = 0.025$), E1 ($P = 0.004$), E2 ($P = 0.0066$) (PGA2, PGB2, PGE1, PGE2, respectively), and thromboxane B2 ($P = 0.002$) occur in MIBC in contrast to both normal urothelium and NMIBC (Fig. 6), whereas PGD2, PGI2, and 6-keto prostaglandin F1alpha were significantly decreased in urothelial carcinoma in contrast to normal urothelium (data not shown). These findings suggest that urothelial carcinomas that are at least T2 in nature show enhanced COX, prostaglandin synthase E, and thromboxane synthase pathways and repressed prostaglandin synthase D and prostacyclin synthase pathways. In addition, increased arachidonate metabolism occurs in MIBC, with evidence of elevated 5-HETE ($P = 0.0747$) and 15-HETE ($P = 0.0147$).

MIBC derives NAD⁺ from tryptophan instead of the salvage pathway

NAD⁺ is produced either by de novo synthesis from tryptophan or the salvage pathway from nicotinamide and nicotinate. Elevated kynurenine ($P = 0.0212$), anthranilate ($P = 0.0111$), and quinolate ($P = 0.0015$) in MIBC indicate that de novo synthesis of NAD⁺ occurs in MIBC

(Fig. 7). This may be influenced by local TNF-alpha and INF-gamma production by local inflammatory cells and requires further investigation [16]. Furthermore, the salvage pathway for NAD⁺ synthesis appears defective in MIBC, evidenced by reduced levels of NMN ($P = 0.0239$), NAD⁺ ($P = 0.0062$), and NADH ($P = 0.0007$).

Hemoglobin catabolites are increased in MIBC

The hemoglobin catabolite bilirubin was significantly higher in MIBC ($P = 0.0001$ for bilirubin (Z,Z) and $P = 0.0069$ for bilirubin (E,E)), suggesting enhanced heme catabolism in higher stage tumors.

Discussion

Metabolomics is an emerging “omics” technology which gives information about the sum total of all metabolites within a biological sample which represents the end result of biological processes as a manifestation of its genetic information. It is a functional readout of the tissue biochemistry that better mirrors the phenotypic state as compared to other approaches such as transcriptomics and proteomics. The application of metabolomic analysis in bladder cancer has primarily focused on the distinction between normal-appearing urothelium and bladder cancer tissue and on the identification of bladder cancer using serum and urine samples [5, 6]. We have expanded upon studies in the literature by including the analysis of urothelial carcinomas in different stage categories, using the distinction between NMIBC and MIBC as a primary stratifier given the unique treatment modalities for these two populations. We confirmed unique pathway alterations that differentiate normal-appearing urothelium from urothelial carcinoma in two different cohorts and secondarily stratified metabolomic data between NMIBC and MIBC. Many major metabolic pathways were altered between normal-appearing urothelium and urothelial carcinoma, whereas a more limited metabolite profile distinguished NMIBC from MIBC.

Metabolites associated with cellular energy status were frequently altered in urothelial carcinoma. Preferential use of glucose for glycolysis and sorbitol production was identified in urothelial carcinoma and is indicative of the Warburg phenomenon that is common in cancer [11]. Anaplerosis, a mechanism to replenish TCA cycle intermediates such as oxaloacetate, alpha-ketoglutarate, succinyl-CoA, and fumarate from substrates such as amino acids and fatty acids [17], also appears to occur in urothelial carcinoma to maintain energy status in cancer cells. Evidence in support of anaplerotic activity includes elevation of late-stage TCA intermediates, increased amino acid metabolites such as succinylcarnitine and

Increased prostaglandin, thromboxane and arachidonate metabolism in muscle invasive urothelial carcinoma

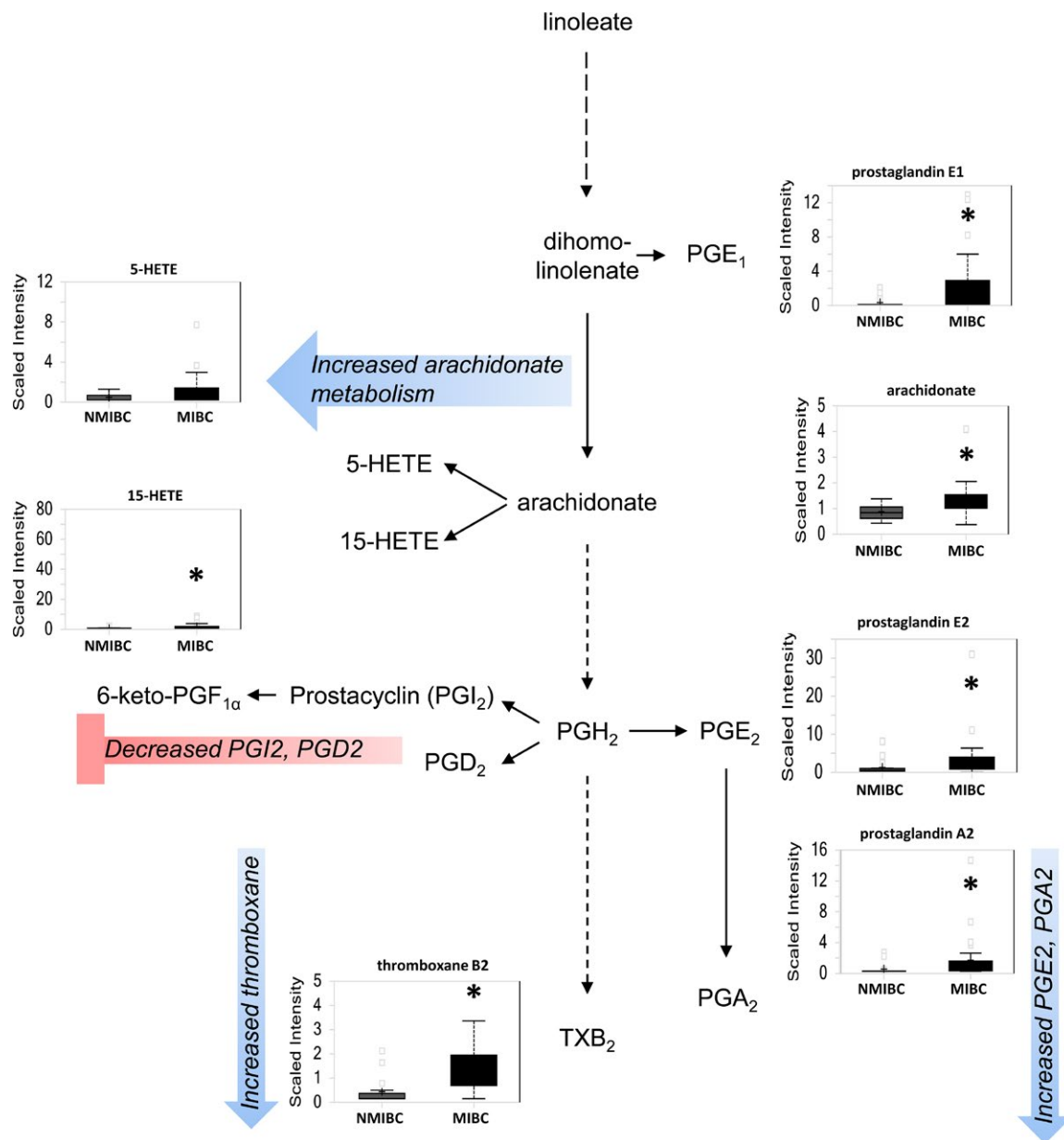


Figure 6. Eicosanoid metabolism is preferentially increased in MIBC as compared to NMIBC. The de novo pathway of NAD⁺ synthesis is enhanced, whereas the salvage pathway is repressed in more advanced urothelial carcinoma. Increased activity of COX and LOX pathways suggests a potential role for inflammatory mediators in MIBC.

propionylcarnitine, and increased fatty acid beta-oxidation to generate acetyl-CoA and succinyl-CoA.

Increased production of the majority of lipid classes occurs in urothelial carcinoma and can influence numerous cancer-related processes that include membrane formation, energy metabolism precursors, and cellular signaling [18]. Increased lipid classes may occur through

several mechanisms. One mechanism is increased biosynthesis from citrate, which has been reported to be increased in urothelial carcinoma [11]. A second mechanism to increase lipid levels is an increased rate of lipid membrane turnover and membrane remodeling that may occur secondary to increased cancer cell proliferation. Finally, inflammatory infiltrates may also induce cancer cell lipid

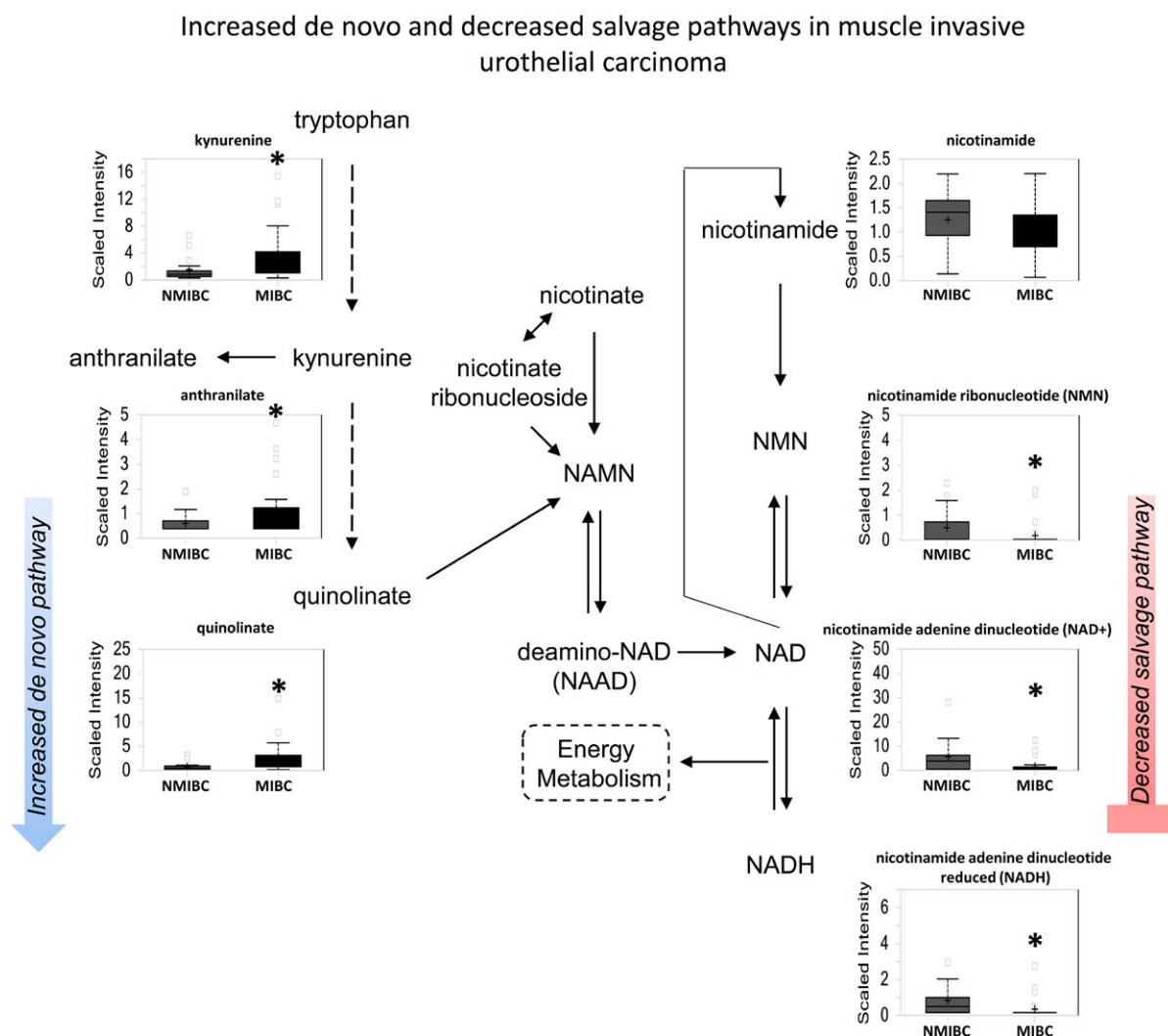


Figure 7. NAD⁺ metabolism is elevated in MIBC as compared with NMIBC. The de novo pathway of NAD⁺ synthesis is enhanced, whereas the salvage pathway is repressed in more advanced urothelial carcinoma. Increased levels of kynurenine, 3-hydroxykynurenine, and quinolinate suggest a potential role for inflammatory mediators in MIBC.

membrane turnover, resulting in higher levels of fatty acids [18]. In our study, elevation in lysolipid levels in urothelial carcinoma may support a role for membrane turnover in lipid elevation, rather than derivation from citrate.

We also identified changes in sphingolipid metabolism in urothelial carcinoma. Specifically, increased sphingosine and reduced sphingomyelin formation in cancer is consistent with activity of sphingosine-1-phosphate that has been implicated in cancer growth [19]. Decreases in sphingomyelin intermediates seen in urothelial carcinoma may occur secondary to increased sphingomyelin breakdown, decreased sphingomyelin synthesis, or increased microvesicle formation in carcinoma, with the latter reported to critically alter tumor biology by regulating cell-to-cell

communication and influence invasion, inflammation, expansion, etc [20]. As significant advances in sphingolipid-based cancer therapeutics have been reported [21], further analysis of this pathway in urothelial carcinoma therapeutics may be warranted.

Finally, we identified several changes of relevance to nucleotide synthesis in urothelial carcinoma relative to normal-appearing urothelium. Shunting of glucose to the PPP produces ribose 5-phosphate, a major 5-sugar moiety required for nucleotide synthesis [22]. We also identified increased purine and pyrimidine pathway intermediates in urothelial carcinoma. When combined with data from energy pathways, this suggests that proliferative capacity in urothelial carcinoma is likely fueled through both glucose and TCA cycle intermediate catabolism.

Table 3. Selected list of potential actionable targets in urothelial carcinoma identified by metabolomic analysis.

Pathway	Target molecule	Agent
PPAR	PPAR γ	Thiazolidinediones
	Dual PPAR γ and PPAR α	(Rosiglitazone, Pioglitazone), Muraglitazar, Tesaglitazar
Sphingolipid	Glucosyl ceramide synthase	PPMP, PPPP, etc.
	Sphingosine kinase	SKi, DHS, etc.
	Sphingosine 1-phosphate receptor	FTY-720, LT1002, etc.
	Ceramidase	D-MAPP, B13, etc.
Eicosanoid	LOX-5	AA861
	COX-2	Celecoxib, Rofecoxib
	Dual COX-2 and COX-1	NSAIDs (ibuprofen, aspirin, etc.)
	Dual LOX-5 and COX-2	Licofelone
Heme	HO-1	Metalloporphyrins (ZnPP, SnMP etc.)
		Imidazole derivatives (Azalanstat, OB-24)

We next compared metabolite differences between high-grade NMIBC and MIBC, an analysis that is unique to our metabolomic study on urothelial carcinoma. Although these broad classification categories encompass carcinomas at different stages and thus in the progression spectrum of urothelial carcinoma, we selected this stratification based on the distinct treatment approaches between these two categories and the need for alternative therapies specific to these two settings. Three major pathways were uniquely altered in MIBC and included increased eicosanoid signaling, enhanced use of de novo synthesis of NAD⁺ for energy and DNA repair, and increased heme catabolism.

Altered eicosanoid metabolites seen in MIBC suggest an increase in both COX and LOX activity, with alterations in numerous metabolites in these pathways. These pathways have been implicated in inflammatory cell regulation, tumorigenesis, cell proliferation, and angiogenesis and represent potential actionable pathways in urothelial carcinoma [23–25]. The COX pathway can have mixed effects on tumorigenesis, with COX and PGE2 implicated in pro-tumorigenic activity, whereas PGD2 and PGI2 may have anti-tumorigenic activities [26, 27]. Increased LOX-mediated arachidonate metabolism was also evident in our study and is supported by a recent description of increased 5-LOX in urothelial carcinoma relative to normal urothelium [23]. 5-LOX activity is essential for urothelial carcinoma cell growth and requires the 5-LOX product 5-HETE [24], which we also identified as increased in MIBC.

We also found increased NAD⁺ de novo synthesis in MIBC and prior reports have suggested that cancers highly dependent on NAD⁺ can use this metabolite as a cofactor for the DNA repair enzyme PARP [28]. Finally, elevated levels of hemoglobin catabolites were identified in MIBC, with putative increased heme oxygenase-1 (HO-1) activity responsible for increased heme cleavage to biliverdin and ultimately bilirubin. HO-1 upregulation occurs in cancer and regulates oncogenic factors, such as matrix metalloproteinase (MMP) family members and vascular endothelial growth factor (VEGF) [25]. HO-1 is also upregulated by smoking, a major risk factor for urothelial carcinoma [29]. Although no HO-1 targeting drugs are currently available, many novel HO-1 inhibitors are being developed and may be of relevance to urothelial carcinoma [30].

Two major effectors that could influence regulation of these multiple pathways in parallel include both p53 activity and associated inflammation. Although analysis of these two mechanisms was beyond the scope of the current analysis, both factors could potentially play a significant role in coordinating the metabolic changes we have identified. The tumor-suppressor p53 is frequently mutated in bladder cancer [3, 11] and can regulate glucose metabolism, lipid metabolism, oxidative stress, proline oxidase expression, and apoptosis through effects on peroxisome proliferator-activated receptor gamma (PPAR- γ) [12, 13, 31, 32]. Inflammation has also been implicated in cancer cell behavior, and we have identified several alterations that suggest inflammation status may impact changes in urothelial carcinoma. Specifically, pathway alterations present in fatty acid production, proline synthesis, NAD⁺ synthesis, and heme catabolism can all be directionally regulated by inflammatory cells [33–36]. Given that the vast majority of patients in this study are BCG-naïve, many of these effects may relate to underlying tumor cell and/or stromal factors and appear to be especially pronounced in MIBC [37].

We compared our results to two prior studies, which have primarily focused on the distinction between benign and cancerous tissue, rather than stage or progression. Putluri et al. [8] identified 35 biochemicals differentiating benign and tumor. We identified all but eight of these. Of those that were present, 19 showed similar directional change, one was unaltered and seven showed opposite directional change. Tripathi et al. [4] identified eight differential metabolites between normal and tumor using nuclear magnetic resonance. All of them showed the same directional change in our study. In contrast to their study, which did not find differences between pTa/pT1 and >pT2 tumors, our analysis revealed several significantly altered metabolites. Furthermore, in contrast to both studies, our analysis, through the utilization of an unbiased global biochemical profiling LC/MS and GC/MS based platform

employing a biochemical library of greater than 2000 known biochemicals, resulted in the detection of hundreds of significantly altered metabolites that are consistent with the cancer phenotype reported both in bladder cancer and other solid tumors. One limitation in all studies that employ normal-appearing (“benign”) urothelium in analysis of bladder cancer patients is that preneoplastic molecular alterations may be present without affecting the morphological appearance of the urothelium. Given that all studies evaluating normal-appearing urothelium and bladder carcinoma to date have identified similar alterations in numerous metabolite categories, this limitation may be less critical. Our study has also expanded on prior analyses to include more than one patient cohort and to analyze differences in metabolites between NMIBC and MIBC. We also compared our results to a recent bladder cancer urine study which reported six biomarkers that differentiated cancer and noncancer samples [5]. Three of them had the same directional change in our study, which suggests that changes in these metabolites are due to cancer. Based on these analyses, several potential novel therapeutics approaches can be proposed pending further analysis (Table 3).

Limitations of our study include small numbers of Cohort 1 samples which did not allow for NMIBC versus MIBC comparisons and lack of matched urine samples. Despite these limitations, however, the data maintain robustness across two cohorts with minor metabolite shifts. Follow-up studies that incorporate larger patient cohorts using matched samples and functional testing would be necessary to confirm our results. Correlation of metabolomics data with smoking status, p53 expression, treatments, and outcomes would be valuable. Use of other complementary –omics analyses with metabolomics would provide greater information. Review of TCGA data suggests that many of our altered pathways may also show dysregulation at the transcriptomic level. Studies using a single patient dataset that evaluates both signatures concordantly, combined with functional studies, may be better to assess whether transcriptional changes are responsible for metabolic pathway alterations. We also did not have adequate amounts of carcinoma in situ (Cis) frozen samples and future studies which include adequate volumes of these samples can further elaborate on changes in this group.

In conclusion, we used a highly sensitive metabolomics approach to identify multiple metabolomic pathway changes in urothelial carcinoma. Both glycolysis and anaplerosis appear to be important mechanisms to maintain energy status in urothelial carcinoma. MIBC appears to be distinct in its enhanced signaling through COX and LOX pathways, NAD⁺ synthesis regulation, and heme catabolism. Many of the differential pathways suggest unique actionable approaches to NMIBC and MIBC, pending further investigation.

Conflict of Interest

BW is an employee and BN is a retired employee of Metabolon Inc.

References

1. Ferlay, J., I. Soerjomataram, R. Dikshit, S. Eser, C. Mathers, M. Rebelo, et al. 2015. Cancer incidence and mortality worldwide: sources, methods and major patterns in GLOBOCAN 2012. *Int. J. Cancer* 136:E359–E386.
2. Siegel, R. L., K. D. Miller, and A. Jemal. 2015. Cancer statistics, 2015. *CA Cancer J. Clin.* 65:5–29.
3. Kamat, A. M., and P. Mathew. 2011. Bladder cancer: imperatives for personalized medicine. *Oncology (Williston Park)* 25:951–958, 960.
4. Tripathi, P., B. S. Somashekar, M. Ponnusamy, A. Gursky, S. Dailey, P. Kunju, et al. 2013. HR-MAS NMR tissue metabolomic signatures cross-validated by mass spectrometry distinguish bladder cancer from benign disease. *J. Proteome Res.* 12:3519–3528.
5. Wittmann, B. M., S. M. Stirdivant, M. W. Mitchell, J. E. Wulff, J. E. McDunn, Z. Li, et al. 2014. Bladder cancer biomarker discovery using global metabolomic profiling of urine. *PLoS ONE* 9:e115870.
6. Bansal, N., A. Gupta, N. Mitash, P. S. Shakyia, A. Mandhani, A. A. Mahdi, et al. 2013. Low- and high-grade bladder cancer determination via human serum-based metabolomics approach. *J. Proteome Res.* 12:5839–5850.
7. Dettmer, K., F. C. Vogl, A. P. Ritter, et al. 2013. Distinct metabolic differences between various human cancer and primary cells. *Electrophoresis* 34:2836–2847.
8. Putluri, N., A. Shojaiie, V. T. Vasu, S. K. Vareed, S. Nalluri, V. Putluri, et al. 2011. Metabolomic profiling reveals potential markers and bioprocesses altered in bladder cancer progression. *Cancer Res.* 71:7376–7386.
9. von Rundstedt, F. C., K. Rajapakshie, J. Ma, J. M. Arnold, J. Gohlke, V. Putluri, et al. 2016. Integrative Pathway Analysis of Metabolic Signature in Bladder Cancer: a Linkage to The Cancer Genome Atlas Project and Prediction of Survival. *J. Urol.* 195:1911–1919.
10. Gupta, S., A. M. Hau, J. R. Beach, J. Harwalker, E. Mantuano, S. L. Gonias, et al. 2013. Mammalian target of rapamycin complex 2 (mTORC2) is a critical determinant of bladder cancer invasion. *PLoS ONE* 8:e81081.
11. Levine, A. J., and A. M. Puzio-Kuter. 2010. The control of the metabolic switch in cancers by oncogenes and tumor suppressor genes. *Science* 330:1340–1344.
12. Pandhare, J., S. P. Donald, S. K. Cooper, and J. M. Phang. 2009. Regulation and function of proline oxidase under nutrient stress. *J. Cell. Biochem.* 107:759–768.

13. Liu, Y., G. L. Borchert, S. P. Donald, B. A. Diwan, M. Anver, and J. M. Phang. 2009. Proline oxidase functions as a mitochondrial tumor suppressor in human cancers. *Cancer Res.* 69:6414–6422.
14. Porcelli, B., L. F. Muraca, B. Frosi, E. Marinello, R. Vernillo, A. De Martino, et al. 1997. Fast-atom bombardment mass spectrometry for mapping of endogenous methylated purine bases in urine extracts. *Rapid Commun. Mass Spectrom.* 11:398–404.
15. Klaunig, J. E., L. M. Kamendulis, and B. A. Hocevar. 2010. Oxidative stress and oxidative damage in carcinogenesis. *Toxicol. Pathol.* 38:96–109.
16. Chiarugi, A., M. Calvani, E. Meli, E. Traggiai, and F. Moroni. 2001. Synthesis and release of neurotoxic kynurenine metabolites by human monocyte-derived macrophages. *J. Neuroimmunol.* 120:190–198.
17. Owen, O. E., S. C. Kalhan, and R. W. Hanson. 2002. The key role of anaplerosis and cataplerosis for citric acid cycle function. *J. Biol. Chem.* 277:30409–30412.
18. Cerne, D., I. P. Zitnik, and M. Sok. 2010. Increased fatty acid synthase activity in non-small cell lung cancer tissue is a weaker predictor of shorter patient survival than increased lipoprotein lipase activity. *Arch. Med. Res.* 41:405–409.
19. Ponnusamy, S., M. Meyers-Needham, C. E. Senkal, S. A. Saddoughi, D. Sentelle, S. P. Selvam, et al. 2010. Sphingolipids and cancer: ceramide and sphingosine-1-phosphate in the regulation of cell death and drug resistance. *Future Oncol.* 6:1603–1624.
20. Muralidharan-Chari, V., J. W. Clancy, A. Sedgwick, and C. D'Souza-Schorey. 2010. Microvesicles: mediators of extracellular communication during cancer progression. *J. Cell Sci.* 123:1603–1611.
21. Adan-Gokbulut, A., M. Kartal-Yandim, G. Iskender, and Y. Baran. 2013. Novel agents targeting bioactive sphingolipids for the treatment of cancer. *Curr. Med. Chem.* 20:108–122.
22. Tong, X., F. Zhao, and C. B. Thompson. 2009. The molecular determinants of de novo nucleotide biosynthesis in cancer cells. *Curr. Opin. Genet. Dev.* 19:32–37.
23. Madka, V., A. Mohammed, Q. Li, Y. Zhang, J. M. Patlolla, L. Biddick, et al. 2014. Chemoprevention of urothelial cell carcinoma growth and invasion by the dual COX-LOX inhibitor licoferone in UPII-SV40T transgenic mice. *Cancer Prev. Res. (Phila.)* 7:708–716.
24. Hayashi, T., K. Nishiyama, and T. Shirahama. 2006. Inhibition of 5-lipoxygenase pathway suppresses the growth of bladder cancer cells. *Int. J. Urol.* 13:1086–1091.
25. Miyata, Y., S. Kanda, K. Mitsunari, A. Asai, and H. Sakai. 2014. Heme oxygenase-1 expression is associated with tumor aggressiveness and outcomes in patients with bladder cancer: a correlation with smoking intensity. *Transl. Res.* 164:468–476.
26. Keith, R. L., Y. E. Miller, T. M. Hudish, C. E. Giron, S. Sotto-Santiago, W. A. Franklin, et al. 2004. Pulmonary prostacyclin synthase overexpression chemoprevents tobacco smoke lung carcinogenesis in mice. *Cancer Res.* 64:5897–5904.
27. Kim, J., P. Yang, M. Suraokar, A. L. Sabichi, N. D. Llansa, G. Mendoza, et al. 2005. Suppression of prostate tumor cell growth by stromal cell prostaglandin D synthase-derived products. *Cancer Res.* 65:6189–6198.
28. Weaver, A. N., and E. S. Yang. 2013. Beyond DNA Repair: additional Functions of PARP-1 in Cancer. *Front Oncol.* 3:290.
29. Besaratinia, A., and S. Tommasi. 2013. Genotoxicity of tobacco smoke-derived aromatic amines and bladder cancer: current state of knowledge and future research directions. *FASEB J.* 27:2090–2100.
30. Motterlini, R., and R. Foresti. 2014. Heme oxygenase-1 as a target for drug discovery. *Antioxid. Redox Signal.* 20:1810–1826.
31. Liang, Y., J. Liu, and Z. Feng. 2013. The regulation of cellular metabolism by tumor suppressor p53. *Cell Biosci.* 3:9.
32. Kim, K. Y., J. H. Ahn, and H. G. Cheon. 2007. Apoptotic action of peroxisome proliferator-activated receptor-gamma activation in human non small-cell lung cancer is mediated via proline oxidase-induced reactive oxygen species formation. *Mol. Pharmacol.* 72:674–685.
33. Tamma, S. M., B. Shorter, K. L. Toh, R. Moldwin, and B. Gordon. 2015. Influence of polyunsaturated fatty acids on urologic inflammation. *Int. Urol. Nephrol.* 47:1753–1761.
34. Gecit, I., M. Aslan, M. Gunes, N. Pirincci, R. Esen, H. Demir, et al. 2012. Serum prolidase activity, oxidative stress, and nitric oxide levels in patients with bladder cancer. *J. Cancer Res. Clin. Oncol.* 138:739–743.
35. Surjana, D., G. M. Halliday, and D. L. Damian. 2010. Role of nicotinamide in DNA damage, mutagenesis, and DNA repair. *J. Nucleic. Acids* 2010:157591, 13 pages.
36. Chau, L. Y. 2015. Heme oxygenase-1: emerging target of cancer therapy. *J. Biomed. Sci.* 22:22.
37. Sucher, R., K. Kurz, G. Weiss, R. Margreiter, D. Fuchs, and G. Brandacher. 2010. IDO-Mediated Tryptophan Degradation in the Pathogenesis of Malignant Tumor Disease. *Int. J. Tryptophan Res.* 3:113–120.

Supporting Information

Additional supporting information may be found in the online version of this article:

Figure S1. Immunoblot validation of glucose metabolism enzymes shows altered protein levels that correspond to metabolomics data. Benign UROtsa and invasive T24, J82, and UM-UC-3 cell lines are shown.